ARMY RESEARCH LABORATORY

Propagation of Electromagnetic Fields Over Flat Earth

Joseph R. Miletta

ARL-TR-2352 February 2001

Army Research Laboratory

Adelphi, MD 20783-1197

ARL-TR-2352 **February 2001**

Propagation of Electromagnetic Fields Over Flat Earth

Joseph R. Miletta

Sensors and Electron Devices Directorate

Abstract

This report looks at the interaction of radiated electromagnetic fields with earth ground in military or law-enforcement applications of high-power microwave (HPM) systems. For such systems to be effective, the microwave power density on target must be maximized. The destructive and constructive scattering of the fields as they propagate to the target will determine the power density at the target for a given source. The question of field polarization arises in designing an antenna for an HPM system. Should the transmitting antenna produce vertically, horizontally, or circularly polarized fields? Which polarization maximizes the power density on target? This report provides a partial answer to these questions. The problems of calculating the reflection of uniform plane wave fields from a homogeneous boundary and calculating the fields from a finite source local to a perfectly conducting boundary are relatively straightforward. However, when the source is local to a general homogeneous plane boundary, the solution cannot be expressed in closed form. An approximation usually of the form of an asymptotic expansion results. Calculations of the fields are provided for various source and target locations for the frequencies of interest. The conclusion is drawn that the resultant vertical field from an appropriately oriented source antenna located near and above the ground can be significantly larger than a horizontally polarized field radiated from the same location at a 1.3 GHz frequency at observer locations near and above the ground.

Contents

1 Introduction **1**

2 Problem Formulation **2**

2.1 Vertical Dipole Over Earth 3

2.2 Horizontal Dipole Over Earth 4

2.3 Comparisons 5

2.3.1 Comparison of Field Components Near the Earth . . 6

3 Conclusion **14**

References **15**

Appendix. MATLAB® m-Files **17**

Distribution **27**

Report Documentation Page **29**

Figures

1 Geometry for vertical and horizontal dipole formulations 2

2 Comparison of main electric field components from a vertical (E_z) and from a horizontal (E_ϕ) broadside ideal dipole over a perfectly conducting ground 7

3 Reflection coefficients for vertically and horizontally polarized plane waves of 1.3-GHz frequency incident on a flat ground for five earth-parameter cases listed in table 1 8

4 Fresnel reflection coefficient for a vertically polarized plane wave field compared to "reflection coefficient" as calculated by complete formulation for a vertical dipole over homogeneous earth as observed at 1-m height 1000 m down range at a frequency of 1.3 GHz 9

5 Fresnel reflection coefficient for a horizontally polarized plane wave field compared to "reflection coefficient" as calculated by complete formulation for a horizontal dipole over homogeneous earth as observed at 1-m height, broadside 1000 m down range at a frequency of 1.3 GHz 10

6 Comparison of principal fields from an ideal dipole oriented perpendicular and horizontal to a homogeneous flat earth . . . 11
7 Comparison of principal fields from an ideal dipole oriented perpendicular and horizontal to a homogeneous flat earth . . . 12
8 Effect of ground reflection on primary field components near ground for typical earth parameters 13

Tables

1 Earth parameters 6

1. Introduction

Effective military or law-enforcement applications of high-power microwave (HPM) systems in which the HPM system and the target system are on or near the ground or water require that the microwave power density on target be maximized. The power density at the target for a given source will depend on the destructive and constructive scattering of the fields as they propagate to the target. Antenna design for an HPM system includes addressing the following questions about field polarization: Should the fields the transmitting antenna produces be vertically, horizontally, or circularly polarized? Which polarization maximizes the power density on target? (The question of which polarization best couples to the target is beyond the scope of this report.) While this report does not completely answer these questions, it addresses the interaction of the radiated electromagnetic fields with earth ground. It is assumed that the transmitting antenna and the target (or receiver) are located above, but near the surface of a flat idealized earth (constant permittivity, ε, and conductivity, σ) ground. First an ideal vertical dipole (oriented along the z-axis perpendicular to the ground plane) is addressed. The horizontal dipole (parallel to the ground plane) follows.

2. Problem Formulation

The problems of calculating the reflection of uniform plane wave fields from a homogeneous boundary and calculating the fields from a finite source local to a perfectly conducting boundary are relatively straightforward. However, when the source is local to a general homogeneous plane boundary, it is found that the solution cannot be expressed in closed form. An approximation usually of the form of an asymptotic expansion results. The problem of an ideal dipole over a homogeneous half-space has been the topic of a number of studies starting at the turn of the last century with the solution provided by Sommerfeld (1949) and leading to the more contemporary work of Banos (1966) and King et al (1994, 1992). References such as Maclean and Wu (1993) address in detail the many approaches to solving the problem. Considerable controversy has surrounded these studies. We will not attempt to derive the solution or otherwise discuss the solution of the problem in this report. We will rely on the work of King et al for a complete and concise formulation of the problem. Figure 1 depicts the problem geometry. The King expressions have been encoded and solved in MATLAB® (1984–1999). Comparisons of the field structures are provided for various source and target locations for frequencies of interest.

The expressions that follow are constrained by the magnitude of the wave numbers ($k = \omega(\mu\epsilon)^{1/2}, \omega = 2\pi \times$ frequency) in each region:

$$|k_1| \geq 3\,|k_2| \ , \tag{1}$$

where, after King, the subscript 2 denotes the upper half-space (air) and the subscript 1 denotes the lower half-space (earth). Also, μ is the permeability in henries per meter, ε is the permittivity in farads per meter, and σ is the conductivity in siemens per meter. The subscripts 0 and r represent free space and relative to free space, respectively.

Figure 1. Geometry for vertical and horizontal dipole formulations.

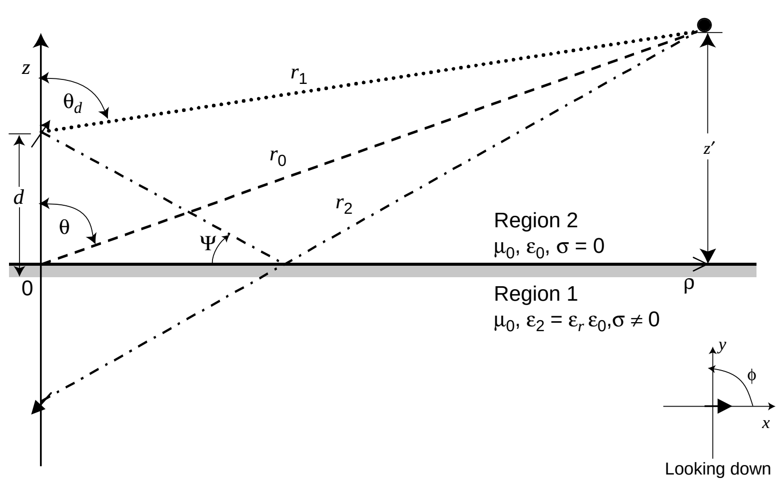

2.1 Vertical Dipole Over Earth

The electromagnetic fields from a dipole with dipole moment $I\ell$ oriented perpendicular to and at a height $z = d$ above the ground plane have three components in cylindrical coordinates. The magnetic field is symmetric about the z-axis, perpendicular to the direction of propagation. For that reason the fields will be termed transverse magnetic (TM) fields. (We will find that the horizontal dipole has TM and transverse electric (TE) components.) The formulation as provided in King et al (1994) is, referring to figure 1,

$$
\begin{aligned}
H_\phi(\rho,z) &= -\frac{I\ell}{2\pi}\left[\begin{array}{l} \frac{e^{ik_2r_1}}{2}\left(\frac{\rho}{r_1}\right)\left(\frac{ik_2}{r_1}-\frac{1}{r_1^2}\right)+\frac{e^{ik_2r_2}}{2}\left(\frac{\rho}{r_2}\right)\left(\frac{ik_2}{r_2}-\frac{1}{r_2^2}\right) \\ -e^{ik_2r_2}\left(\frac{k_2^3}{k_1}\right)\left(\frac{\pi}{k_2r_2}\right)^{\frac{1}{2}}e^{-iP}F(P) \end{array}\right], &(2)\\
E_\rho(\rho,z) &= -\frac{\omega\mu_0 I\ell}{2\pi k_2}\left\{\begin{array}{l} \frac{e^{ik_2r_1}}{2}\left(\frac{\rho}{r_1}\right)\left(\frac{z-d}{r_1}\right)\left(\frac{ik_2}{r_1}-\frac{3}{r_1^2}-\frac{3i}{k_2r_1^3}\right) \\ +\frac{e^{ik_2r_2}}{2}\left(\frac{\rho}{r_2}\right)\left(\frac{z+d}{r_2}\right)\left(\frac{ik_2}{r_2}-\frac{3}{r_2^2}-\frac{3i}{k_2r_2^3}\right) \\ -\frac{k_2}{k_1}e^{ik_2r_2}\left[\left(\frac{\rho}{r_2}\right)\left(\frac{ik_2}{r_2}-\frac{1}{r_2^2}\right)-\left(\frac{k_2^3}{k_1}\right)\left(\frac{\pi}{k_2r_2}\right)^{\frac{1}{2}}e^{-iP}F(P)\right] \end{array}\right\}, \text{ and} &(3)\\
E_z(\rho,z) &= \frac{\omega\mu_0 I\ell}{2\pi k_2}\left\{\begin{array}{l} \frac{e^{ik_2r_1}}{2}\left[\left(\frac{ik_2}{r_1}-\frac{1}{r_1^2}-\frac{i}{k_2r_1^3}\right)-\left(\frac{z-d}{r_1}\right)^2\left(\frac{ik_2}{r_1}-\frac{3}{r_1^2}-\frac{3i}{k_2r_1^3}\right)\right] \\ +\frac{e^{ik_2r_2}}{2}\left[\left(\frac{ik_2}{r_2}-\frac{1}{r_2^2}-\frac{i}{k_2r_2^3}\right)-\left(\frac{z+d}{r_2}\right)^2\left(\frac{ik_2}{r_2}-\frac{3}{r_2^2}-\frac{3i}{k_2r_2^3}\right)\right] \\ -e^{ik_2r_2}\frac{k_2^3}{k_1}\left(\frac{\rho}{r_2}\right)\left(\frac{\pi}{k_2r_2}\right)^{\frac{1}{2}}e^{-iP}F(P) \end{array}\right\}, &(4)
\end{aligned}
$$

where

$$
\begin{aligned}
r_1 &= \left[\rho^2+(z-d)^2\right]^{\frac{1}{2}}, \\
r_2 &= \left[\rho^2+(z+d)^2\right]^{\frac{1}{2}}, &(5)\\
P &= \frac{k_2^3 r_2}{2k_1^2}\left(\frac{k_2r_2+k_1(z+d)}{k_2\rho}\right)^2, &(6)\\
F(P) &= \int_P^\infty \frac{e^{it}}{(2\pi t)^{\frac{1}{2}}}dt = \frac{1}{2}(1+i)-C_2(P)-iS_2(P), &(7)
\end{aligned}
$$

and $C_2(P), S_2(P)$ are the Fresnel integrals as defined in Abramowitz and Stegun (1970). Since

$$
C_2(P)+iS_2(P) = \frac{1}{2}(1+i)-\sqrt{\frac{i}{2}}e^{iP}w\left(\sqrt{iP}\right), \qquad (8)
$$

we have

$$
F(P) = \sqrt{\frac{i}{2}}e^{iP}w\left(\sqrt{iP}\right), \qquad (9)
$$

where $w(z)$, called the plasma dispersion function with complex argument, is a form of the error function defined in Abramowitz and Stegun (1970). A convenient MATLAB® m-file is available for solving the function with complex argument (Chase) and is provided in the appendix. Note that $\sqrt{i}$ can be written as $\frac{(i+1)}{2}$ and that $F(P)$ always appears with e^{-iP}, thus canceling the exponential term in equation (9). This is reflected in the MATLAB® m-files that calculate the fields (provided in the appendix).

The equations have been written such that the direct and reflected components appear first. The last term is referred to as the surface or lateral wave. Often it is called the Norton surface wave from the engineering models he developed in the mid-1930s. The equations reduce to the fields above a perfectly conducting ground when $k_1 \to \infty$; the surface or lateral wave term then goes to zero.

2.2 Horizontal Dipole Over Earth

The electromagnetic fields produced by an ideal dipole oriented at a height $z = d$ above and parallel to the ground plane consist in general of both TM and TE components. The formulation as provided in King et al (1992) for the TM wave components in cylindrical coordinates, referring to figure 1 and the above definitions, is

$$H_\phi(\rho,\phi,z) = \frac{I\ell}{4\pi}\cos\phi \left[\begin{array}{l} e^{ik_2r_1}\left(\frac{z-d}{r_1}\right)\left(\frac{ik_2}{r_1}-\frac{1}{r_1^2}\right) - e^{ik_2r_2}\left(\frac{z+d}{r_2}\right)\left(\frac{ik_2}{r_2}-\frac{1}{r_2^2}\right) \\ +\frac{2k_2}{k_1}e^{ik_2r_2}\left[\begin{array}{l} \frac{ik_2}{r_2}-\frac{1}{r_2^2}-\frac{i}{k_2r_2^3} \\ -\left(\frac{k_2^3}{k_1}\right)\left(\frac{r_2}{\rho}\right)\left(\frac{\pi}{k_2r_2}\right)^{\frac{1}{2}}e^{-iP}F(P) \end{array}\right] \end{array} \right], \tag{10}$$

$$E_\rho(\rho,\phi,z) = \frac{\omega\mu_0 I\ell}{4\pi k_2}\cos\phi \left\{ \begin{array}{l} e^{ik_2r_1}\left[\frac{2}{r_1^2}+\frac{2i}{k_2r_1^3}+\left(\frac{z-d}{r_1}\right)^2\left(\frac{ik_2}{r_1}-\frac{3}{r_1^2}-\frac{3i}{k_2r_1^3}\right)\right] \\ -e^{ik_2r_2}\left\{ \begin{array}{l} \frac{2}{r_2^2}+\frac{2i}{k_2r_2^3}+\left(\frac{z+d}{r_2}\right)^2\left(\frac{ik_2}{r_2}-\frac{3}{r_2^2}-\frac{3i}{k_2r_2^3}\right) \\ -\frac{2k_2}{k_1}\left(\frac{z+d}{r_2}\right)\left(\frac{ik_2}{r_2}-\frac{1}{r_2^2}\right) \\ +\frac{2k_2^2}{k_1^2}\left[\begin{array}{l} \frac{ik_2}{r_2}-\frac{1}{r_2^2}-\frac{i}{k_2r_2^3} \\ -\left(\frac{k_2^3}{k_1}\right)\left(\frac{r_2}{\rho}\right)\left(\frac{\pi}{k_2r_2}\right)^{\frac{1}{2}}e^{-iP}F(P) \end{array}\right] \end{array} \right\} \end{array} \right\}, \text{ and} \tag{11}$$

$$E_z(\rho,\phi,z) = \frac{\omega\mu_0 I\ell}{4\pi k_2}\cos\phi \left\{ \begin{array}{l} -e^{ik_2r_1}\left(\frac{\rho}{r_1}\right)\left(\frac{z-d}{r_1}\right)\left(\frac{ik_2}{r_1}-\frac{3}{r_1^2}-\frac{3i}{k_2r_1^3}\right) \\ +e^{ik_2r_2}\left(\frac{\rho}{r_2}\right)\left(\frac{z+d}{r_2}\right)\left(\frac{ik_2}{r_2}-\frac{3}{r_2^2}-\frac{3i}{k_2r_2^3}\right) \\ -\frac{2k_2}{k_1}e^{ik_2r_2}\left[\left(\frac{\rho}{r_2}\right)\left(\frac{ik_2}{r_2}-\frac{1}{r_2^2}\right)-\frac{k_2^3}{k_1}\left(\frac{\pi}{k_2r_2}\right)^{\frac{1}{2}}e^{-iP}F(P)\right] \end{array} \right\}. \tag{12}$$

The TM fields are zero broadside to the dipole orientation, $\phi = \frac{\pi}{2}$. The TE components are

$$H_\rho(\rho,\phi,z) = \frac{I\ell}{4\pi}\sin\phi \begin{bmatrix} e^{ik_2r_1}\left(\frac{z-d}{r_1}\right)\left(\frac{ik_2}{r_1}-\frac{1}{r_1^2}\right) - e^{ik_2r_2}\left(\frac{z+d}{r_2}\right)\left(\frac{ik_2}{r_2}-\frac{1}{r_2^2}\right) \\ +\frac{2k_2}{k_1}e^{ik_2r_2}\begin{bmatrix} \frac{2}{r_2^2}+\frac{2i}{k_2r_2^3}+\left(\frac{ik_2^2}{k_1\rho}\right)\left(\frac{r_2^2}{\rho^2}\right)\left(\frac{\pi}{k_2r_2}\right)^{\frac{1}{2}}e^{-iP}F(P) \\ +\left(\frac{z+d}{r_2}\right)^2\left(\frac{ik_2}{r_2}-\frac{3}{r_2^2}-\frac{3i}{k_2r_2^3}\right)\end{bmatrix}\end{bmatrix}, \tag{13}$$

$$H_z(\rho,\phi,z) = \frac{I\ell}{4\pi}\sin\phi \begin{bmatrix} e^{ik_2r_1}\left(\frac{\rho}{r_1}\right)\left(\frac{ik_2}{r_1}-\frac{1}{r_1^2}\right) - e^{ik_2r_2}\left(\frac{\rho}{r_2}\right)\left(\frac{ik_2}{r_2}-\frac{1}{r_2^2}\right) \\ +2\left(\frac{\rho}{r_2}\right)e^{ik_2r_2}\begin{Bmatrix} \left(\frac{k_2}{k_1}\right)\left(\frac{z+d}{r_2}\right)\left(\frac{ik_2}{r_2}-\frac{3}{r_2^2}-\frac{3i}{k_2r_2^3}\right) \\ -\left(\frac{k_2}{k_1}\right)^2\begin{bmatrix}\frac{1}{r_2^2}+\frac{3i}{k_2r_2^3}-\frac{3}{k_2^2r_2^4}+ \\ \left(\frac{z+d}{r_2}\right)^2\left(\frac{ik_2}{r_2}-\frac{6}{r_2^2}-\frac{15i}{k_2r_2^3}\right)\end{bmatrix}\end{Bmatrix}\end{bmatrix}, \text{ and} \tag{14}$$

$$E_\phi(\rho,\phi,z) = -\frac{\omega\mu_0 I\ell}{4\pi k_2}\sin\phi \begin{Bmatrix} e^{ik_2r_1}\left(\frac{ik_2}{r_1}+\frac{1}{r_1^2}-\frac{i}{k_2r_1^3}\right) - e^{ik_2r_2}\left(\frac{ik_2}{r_2}-\frac{1}{r_2^2}-\frac{i}{k_2r_2^3}\right) \\ -e^{ik_2r_2}\begin{Bmatrix} -\frac{2k_2}{k_1}\left(\frac{z+d}{r_2}\right)\left(\frac{ik_2}{r_2}-\frac{1}{r_2^2}\right) \\ +\frac{2k_2^2}{k_1^2}\begin{bmatrix}\frac{2}{r_2^2}+\frac{2i}{k_2r_2^3} \\ +\left(\frac{z+d}{r_2}\right)^2\left(\frac{ik_2}{r_2}-\frac{3}{r_2^2}-\frac{3i}{k_2r_2^3}\right)\end{bmatrix} \\ +\left(\frac{2ik_2^4}{k_1^3\rho}\right)\left(\frac{r_2}{\rho}\right)^2\left(\frac{\pi}{k_2r_2}\right)^{\frac{1}{2}}e^{-iP}F(P)\end{Bmatrix}\end{Bmatrix}. \tag{15}$$

These are the predominant fields broadside to the dipole orientation. Here E_ϕ is often termed the horizontal electric field. Again, the equations reduce to the fields above a perfectly conducting ground when $k_1 \to \infty$; the surface or lateral wave term goes to zero.

2.3 Comparisons

The peak power radiated by a unit dipole is given in Collin and Zucker (1969):

$$\mathrm{P} = \frac{k_2^2\zeta_0}{12\pi}, \tag{16}$$

where ζ_0 is the free-space impedance $\left(\sqrt{\frac{\mu_0}{\varepsilon_0}}\right)$. The fields and power density comparisons that follow are normalized to one watt radiated peak power. To obtain the unnormalized quantities, simply multiply the power results by P and the field results by $\mathrm{P}^{\frac{1}{2}}$. The outward component of the complex Poynting vector over a closed surface is

$$1/2\oint_S \underline{E}\times\underline{H}^*\cdot d\underline{S} = -\mathrm{P}_{\text{complex}}, \tag{17}$$

where the negative sign indicates power flow away from the surface. Our interest is in the real part of the power density at the observer (or target) location. In our cylindrical coordinate system for the TM components, this becomes

$$1/2\ \mathrm{Re}\,(\underline{E}\times\underline{H}^*) = 1/2\ \mathrm{Re}\left(\underline{\rho}_0 E_z H_\phi{}^* + \underline{z}_0 E_\rho H_\phi{}^*\right), \tag{18}$$

where $\underline{\rho}_0$ and $\underline{z}_0$ are the unit vectors in cylindrical coordinates. Near the ground, the power flow is predominantly radial with a small z component. And, for the TE components, we have

$$^1\!/\!_2\ \mathrm{Re}\,(\underline{E} \times \underline{H}^*) = {}^1\!/\!_2\ \mathrm{Re}\left(\underline{\rho}_0 E_\phi H_z{}^* - \underline{z}_0 E_\phi H_\rho{}^*\right) . \tag{19}$$

For the vertical dipole, the power density at the observer (on target) will be

$$P_v = {}^1\!/\!_2\left(\mathrm{Re}\,(E_\phi H_z{}^*) + \mathrm{Re}\,(E_\phi H_\rho{}^*)\right) . \tag{20}$$

The horizontal dipole in general will produce a target power density of

$$P_h = {}^1\!/\!_2\left(\{\mathrm{Re}\,(E_\phi H_z{}^*) - \mathrm{Re}\,(E_z H_\phi{}^*)\} + \{\mathrm{Re}\,(E_\rho H_\phi{}^*) - \mathrm{Re}\,(E_\phi H_\rho{}^*)\}\right) . \tag{21}$$

For broadside calculations this becomes

$$P_h = {}^1\!/\!_2\left(\mathrm{Re}\,(E_\phi H_z{}^*) + \mathrm{Re}\,(E_\phi H_\rho{}^*)\right) . \tag{22}$$

The calculations that follow are limited to a frequency of 1.3 GHz (wavelength, λ_0, is 0.23 m) and dipole heights of 1 to 3 m. Observer (target) heights range from 0 to 5 m. The frequency of 1.3 GHz is chosen, since most of the HPM source and antenna design work at ARL is centered around that frequency. The height ranges are chosen to be consistent with ground vehicle source and target applications. Five classes of ground parameters that are representative of distinctly different terrain will be addressed. These five classes are those discussed in King et al (1994) and are given in table 1.

2.3.1 Comparison of Field Components Near the Earth

When thinking about the interaction of electromagnetic waves with the earth's surface, we often view the earth as a perfect conductor. The horizontally polarized field is reflected with the opposite sign of the incident field, leading to a difference or destructively interfered-with field. The vertically polarized field is reflected with the same sign as the incident field, leading to a sum or constructively interfered-with field. Figure 2 compares the resultant primary field components produced from a horizontal and a vertical ideal dipole located at the same point in space over a perfectly conducting ground plane. From these calculations, one might conclude that

Table 1. Earth parameters.

Case		σ,* S/m	ε_r*
1	Sea water	4	80
2	Wet earth	.4	12
3	Dry earth	.04	8
4	Lake water	.004	80
5	Dry sand	.000	2

*The variable name representing σ in the MATLAB m-files is SIGMA and for ε_r it is EPSREL. These variable names appear on many of the figures.

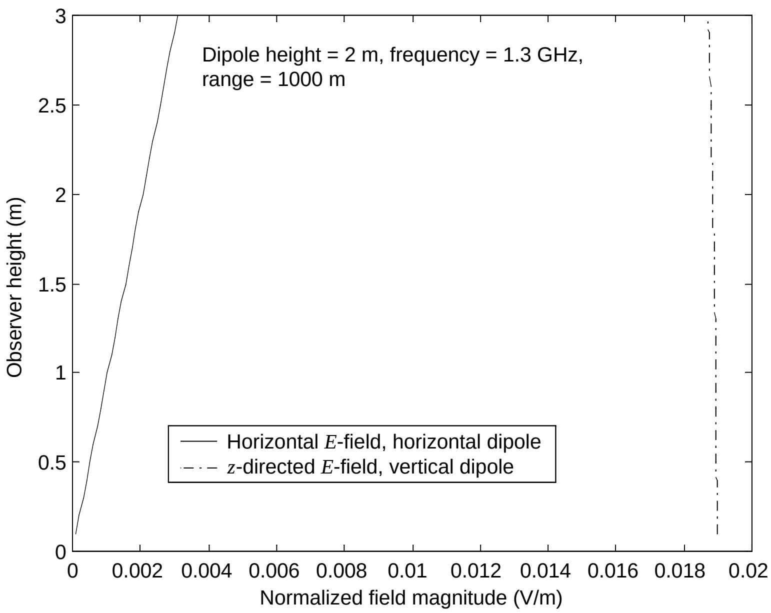

Figure 2. Comparison of main electric field components from a vertical (E_z) and from a horizontal (E_ϕ) broadside ideal dipole over a perfectly conducting ground. E_z is a constructively interfered-with field, while E_ϕ is a destructively interfered-with field.

an antenna that radiated fields polarized such that the electric field was essentially perpendicular to the ground plane would produce the largest fields and, consequently, the greater power densities on a target or near the ground. This is generally not the case for real earth grounds. While the perfectly conducting ground plane model may provide some insight into the interaction with horizontally polarized fields, it clearly is an inadequate model for vertical polarization. The complex reflection coefficients for a plane wave polarized with the electric field in the plane of incidence (vertical polarization) and with a plane wave polarized with the electric field perpendicular to the plane of incidence (horizontal polarization) are given by the following Fresnel expressions. For vertical polarization, it is (Collin, 1985)

$$\rho_{\text{complex}} = \frac{\left(\varepsilon_r - i\frac{\sigma}{\omega\varepsilon_0}\right)\sin\psi - \sqrt{\left(\varepsilon_r - i\frac{\sigma}{\omega\varepsilon_0}\right) - \cos^2\psi}}{\left(\varepsilon_r - i\frac{\sigma}{\omega\varepsilon_0}\right)\sin\psi + \sqrt{\left(\varepsilon_r - i\frac{\sigma}{\omega\varepsilon_0}\right) - \cos^2\psi}} , \tag{23}$$

and for horizontal polarization, it is

$$\rho_{\text{complex}} = \frac{\sin\psi - \sqrt{\left(\varepsilon_r - i\frac{\sigma}{\omega\varepsilon_0}\right) - \cos^2\psi}}{\sin\psi + \sqrt{\left(\varepsilon_r - i\frac{\sigma}{\omega\varepsilon_0}\right) - \cos^2\psi}} , \tag{24}$$

where ψ is the angle of incidence as measured between the ray path and the surface of the earth (see fig. 1). These reflection coefficients for the five cases of table 1 are presented in figure 3. One can clearly see that for shallow grazing angles, a Brewster angle effect exists (often called a pseudo-Brewster angle). The result is destructive interference of the vertically polarized field for incident angles that are less than this pseudo-Brewster

Figure 3. Reflection coefficients for vertically and horizontally polarized plane waves of 1.3-GHz frequency incident on a flat ground for five earth-parameter cases listed in table 1. Note that case 5 provides a true Brewster angle (since conductivity is zero) and case 4 is very near to producing a true Brewster angle at 1.3-GHz frequency: (a) vertical polarization and (b) horizontal polarization.

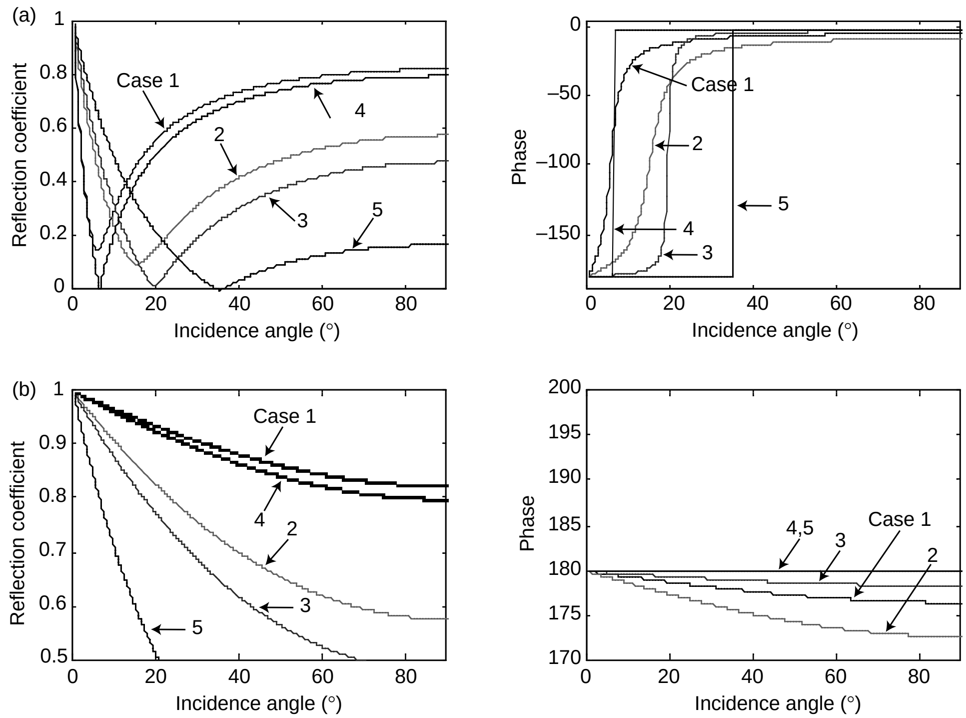

angle. This would lead one to conclude that horizontally and vertically polarized field levels above a ground would be comparable at shallow angles of incidence. The Fresnel equations (22) and (23) do not take into account the surface or lateral wave produced by finite sources above the ground. They are also not applicable to near-field problems. We can compare the reflection coefficients as determined from the Fresnel equations with the results of our complete solution. To do this with the complete equations (eqs (2) to (4) for the vertical dipole and eqs (10) to (15) for the horizontal dipole), we fix the radial (or range) distance to 1000 m. The dipole height is varied to provide a range of incident angles. The observer will be fixed at a 1-m height. The incident and "reflected" fields are

$$E_{\mathrm{vtotal}} = \sqrt{E_\rho^2 + E_z^2}\ , \tag{25}$$

for the vertical dipole and

$$E_{\mathrm{htotal}} = \sqrt{E_\phi^2 + E_\rho^2 + E_z^2}\ , \tag{26}$$

for the horizontal dipole. For broadside calculations, this simply becomes E_ϕ. The terms involving r_1 in equations (2) to (4) and (10) to (15) represent the incident field and the remaining terms represent the reflected and surface wave terms. The reflection coefficient will be calculated as the total incident electric field divided into the total reflected and bound (surface wave) fields. Figures 4 and 5 provide the comparison of the magnitude of the reflection coefficient for the five cases of table 1. For the most part, the Fresnel expressions are a good approximation for the calculation of horizontally polarized field values (fig. 5) above realistic earth ground at

Figure 4. Fresnel reflection coefficient for a vertically polarized plane wave field compared to "reflection coefficient" as calculated by complete formulation for a vertical dipole over homogeneous earth as observed at 1-m height 1000 m down range at a frequency of 1.3 GHz: (a) sea water, (b) wet earth, (c) dry earth, (d) lake water, and (e) dry sand.

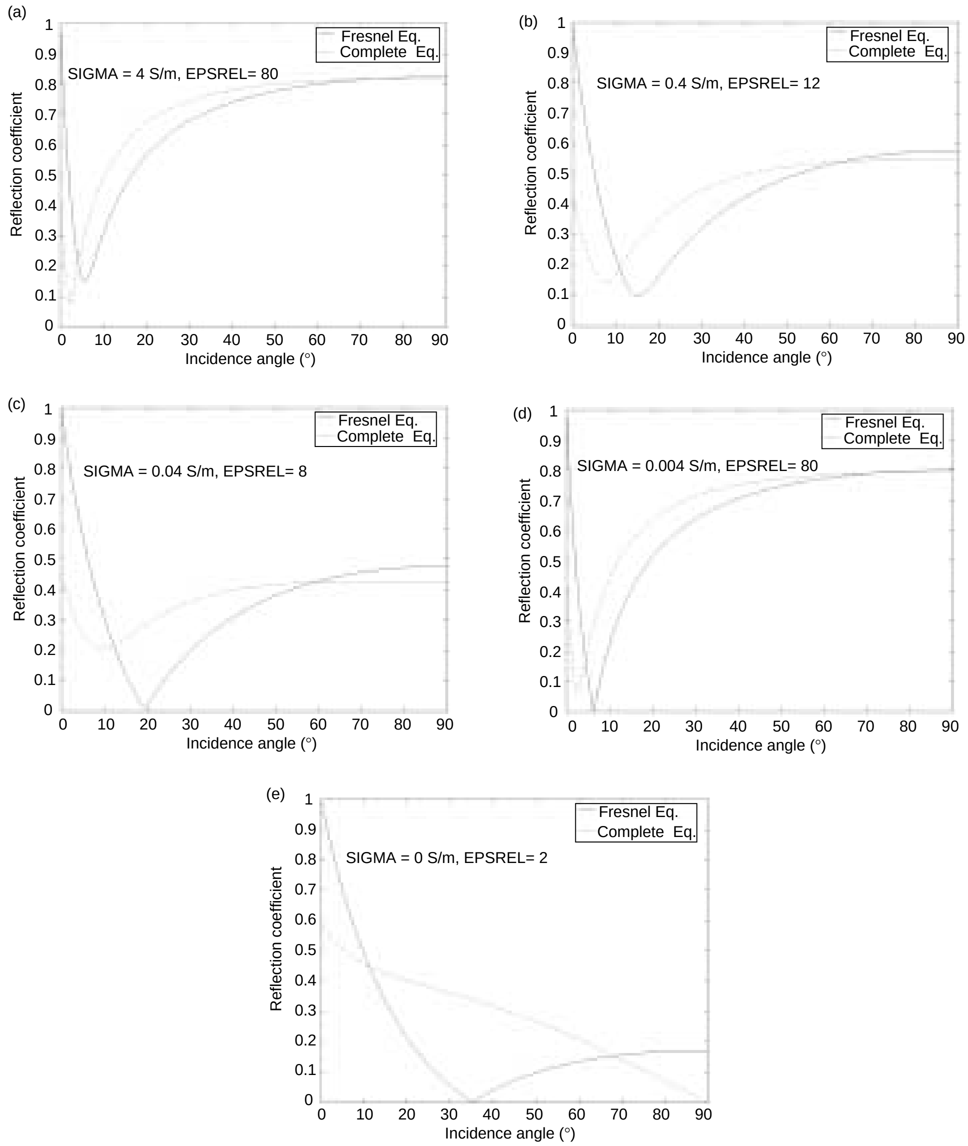

1.3 GHz. The horizontally polarized fields diverge from the Fresnel expressions for low conductivities and relative dielectric constants. The resulting total fields in such cases predicted by the Fresnel expressions will be larger than the complete solution prediction. The results for vertical polarization (fig. 4) show significant divergence for shallow incident angles. In this case the resulting total fields predicted by the complete solution can be significantly higher than that predicted from employing the Fresnel expressions.

Figure 5. Fresnel reflection coefficient for a horizontally polarized plane wave field compared to “reflection coefficient” as calculated by complete formulation for a horizontal dipole over homogeneous earth as observed at 1-m height, broadside 1000 m down range at a frequency of 1.3 GHz: (a) sea water, (b) wet earth, (c) dry earth, (d) lake water, and (e) dry sand.

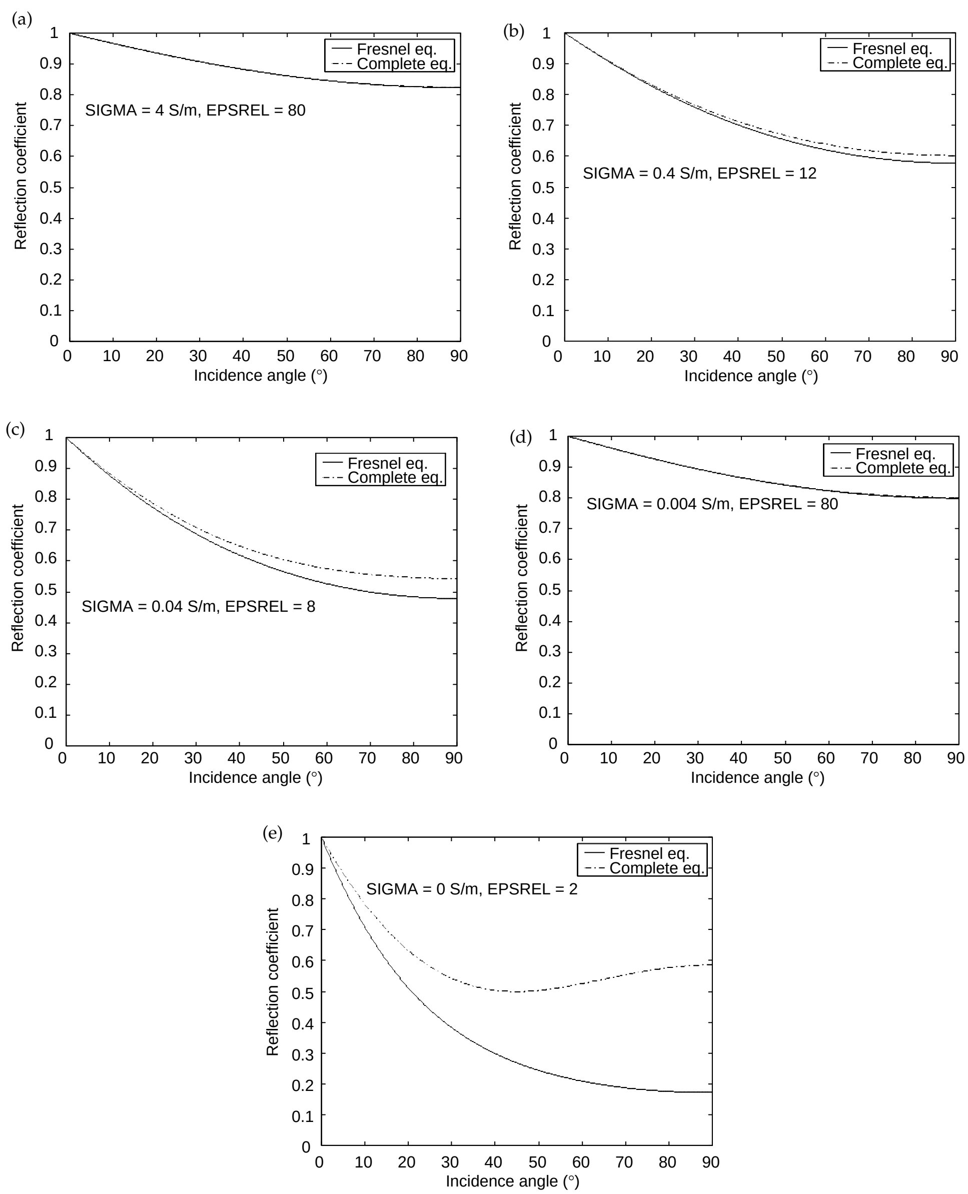

Figures 6 and 7 are plots of the fields produced by the two-dipole orientations; these plots compare the predominant field components for each dipole orientation at 1000 and 100 m, respectively. The plots for the 100-m case (fig. 7) show the beginning of the lobe effect produced by the phase difference between the incident and reflected wave. This is shown more dramatically in figure 8.

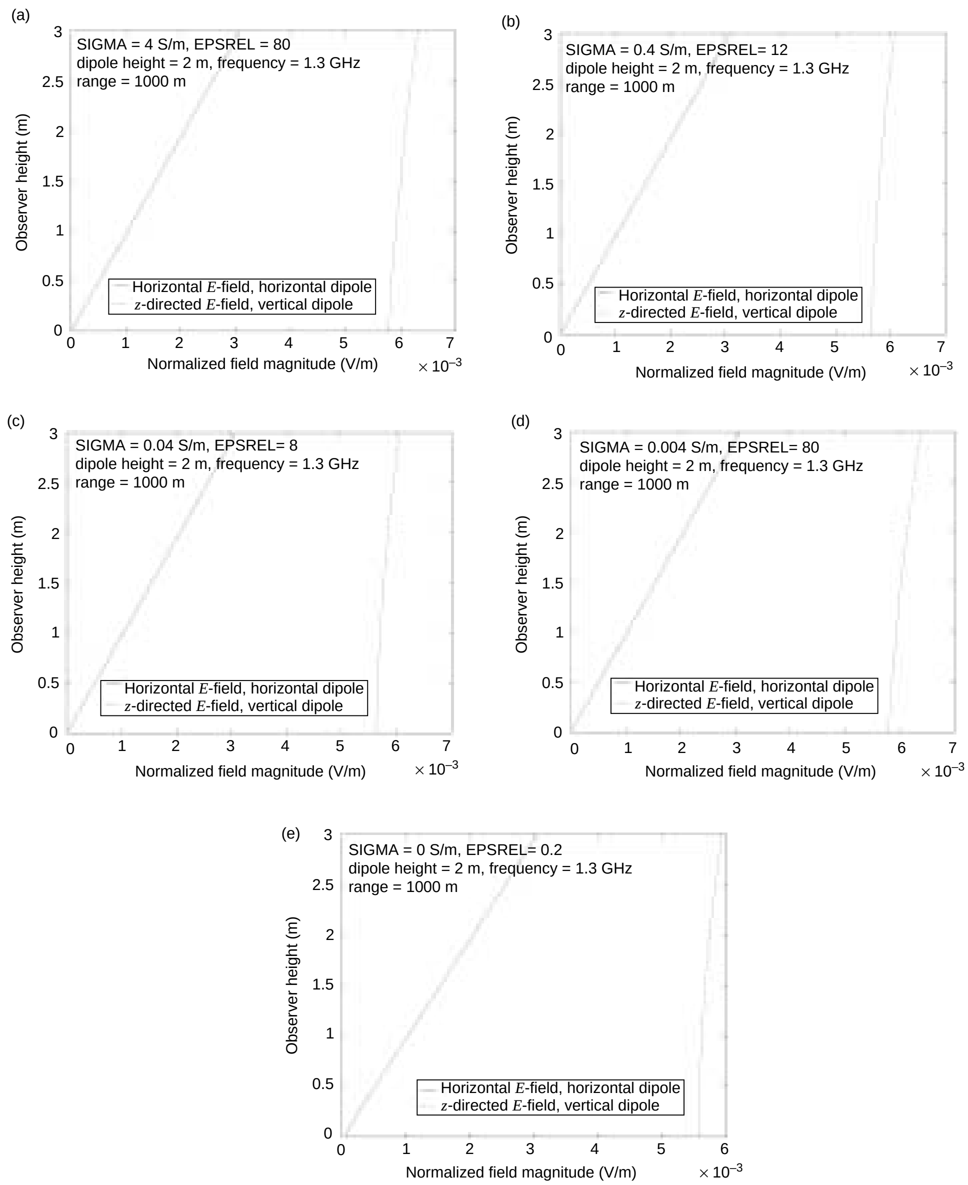

Figure 6. Comparison of principal fields from an ideal dipole oriented perpendicular and horizontal to a homogeneous flat earth. In each case, dipole is placed 2 m above ground plane and observer or target is 1000 m down range: (a) sea water, (b) wet earth, (c) dry earth, (d) lake water, and (e) dry sand.

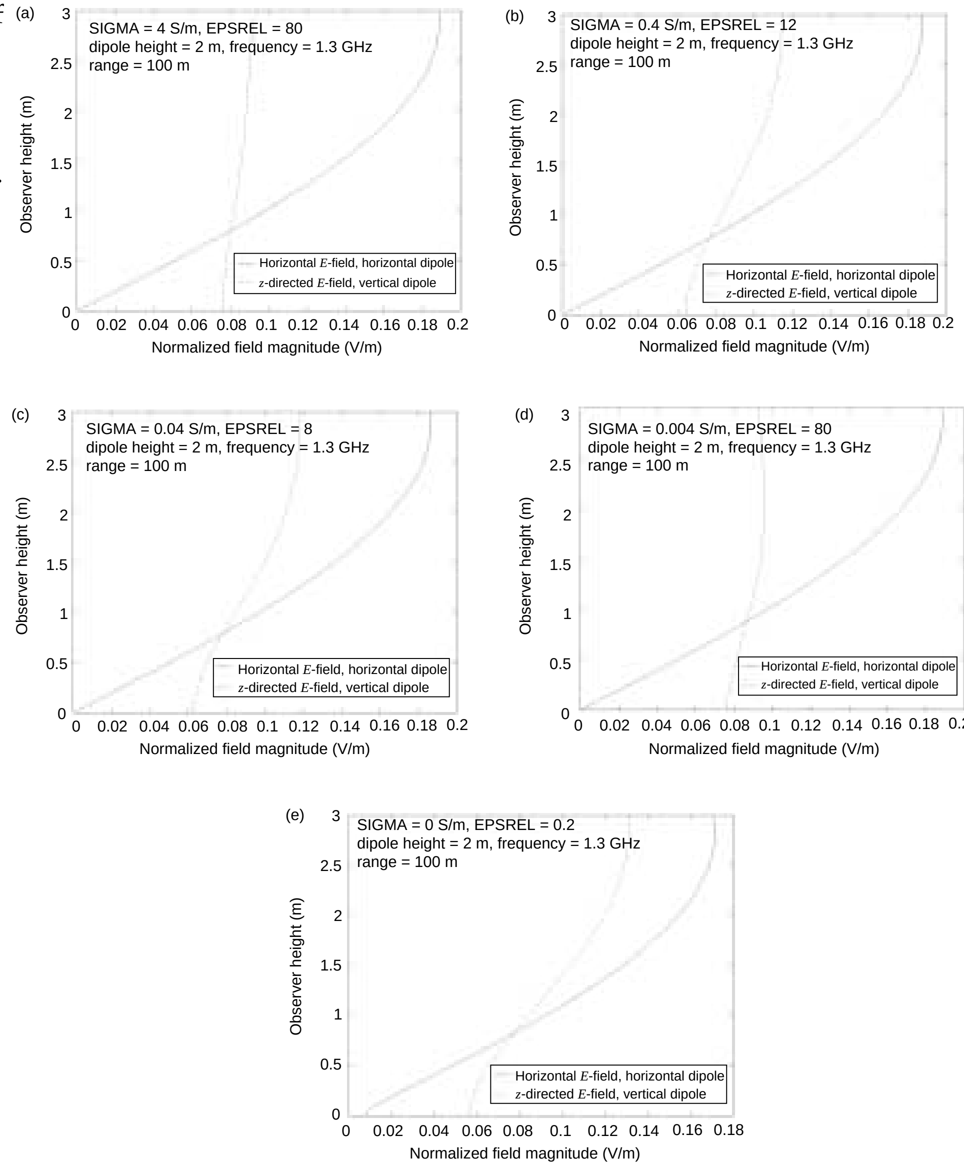

Figure 7. Comparison of principal fields from an ideal dipole oriented perpendicular and horizontal to a homogeneous flat earth. In each case, dipole is placed 2 m above ground plane and observer or target is 100 m down range: (a) sea water, (b) wet earth, (c) dry earth, (d) lake water, and (e) dry sand.

Figure 8. Effect of ground reflection on primary field components near ground for typical earth parameters. Phase difference between incident and reflected waves results in development of field lobes that are more pronounced as radiating antenna is approached: (a) 100 m down range and (b) 1000 m down range.

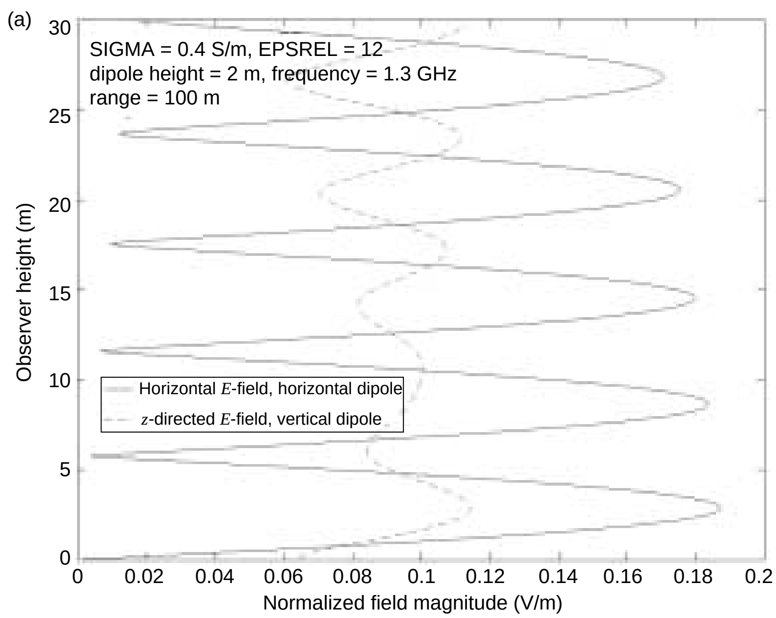

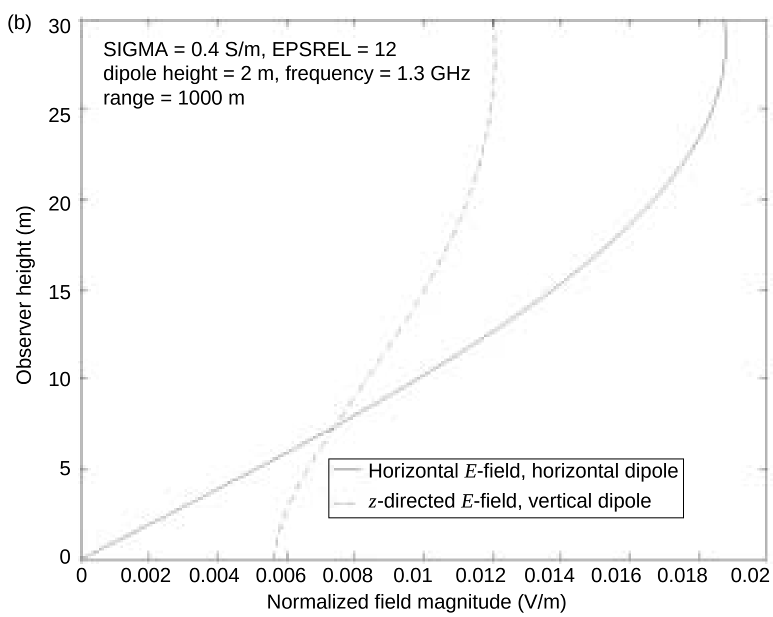

3. Conclusion

A suite of MATLAB® m-files have been developed to calculate the electromagnetic fields produced by a vertical and a horizontal infinitesimal unit dipole over a homogeneous flat (ground) plane. Calculations for the fields above the ground plane have been made for various ground-plane conductivities and relative dielectric constants. The calculations bound the practical range of parameters representative of natural earth terrain.

For a frequency of 1.3 GHz, where the dipole and the observer are close to the ground plane (<3 m), significant difference is seen in the magnitude of the fields from either dipole orientation. The power density on target will be much larger for vertical dipole orientation. The effects of rough terrain, foliage, or scattering from manmade or natural objects in the path from the dipole to target may alter this conclusion. How these other scatterers might affect the field structure at a target at 1.3 GHz is not known at this time. If the effects are random in nature, the present conclusion is most likely still valid. From the simple, smooth, flat ground model, then, one must conclude that vertical polarization (antenna radiating a vertically polarized field) will deliver the most energy to the target. Unless the target's preference for field orientation for maximum pickup is known, a vertically polarized antenna may in fact be the best choice for a ground weapon system.

References

Abramowitz, M., and I. A. Stegun, *Handbook of Mathematical Functions*, National Bureau of Standards, Applied Mathematics Series–55, U.S. Department of Commerce (1970).

Banos, A., *Dipole Radiation in the Presence of a Conducting Half-Space*, Pergamon, Oxford (1966).

Chase, R., MATLAB® m-file, *Plasma Dispersion Function with Complex Argument* (unpublished).

Collin, R. E., *Antenna and Radiowave Propagation*, McGraw-Hill, New York (1985).

Collin, R. E., and F. J. Zucker, *Antenna Theory*, *Part 1*, McGraw-Hill, New York (1969).

King, R.W.P., and S. S. Sandler, "The electromagnetic field of a vertical electric dipole over the earth or sea," IEEE Trans. Antennas Propag. **42**, No. 3 (March 1994), pp 382–389.

King, R.W.P., M. Owens, and T. T. Wu, *Lateral Electromagnetic Waves*, Springer-Verlag, New York (1992).

Maclean, T.S.M., and Z. Wu, *Radiowave Propagation Over Ground*, Chapman and Hall, London (1993).

MATLAB®, release 5.3, The Math Works, Inc., Natick, MA (1984–1999).

Sommerfeld, A., *Partial Differential Equations in Physics*, Academic Press, New York (1949).

Appendix. MATLAB® m-Files

This appendix documents the MATLAB® m-files that implemented the field equations for the vertical and horizontal dipole and array cases. Slight modification may be required to obtain all the calculations presented.

WERF Function

```
function w = werf(z,N)
% WERF(Z,N)   Plasma Dispersion Function with complex argument.
%
% Computes the function w(z)=exp(-z^2)*erfc(-iz) using a rational
% series with N terms.  N should be a power of 2 or it gets SLOW.
% Default value of N is 64.  z can be a matrix of values.
% Taken from Siam Journal on Numerical Analysis, Oct 1994, V31,#5.
% Modified by R. Chase to work for all z (4/3/95).
%
%       N=32 gives approx 14 place accuracy, N=64 is better and
%       it seems as fast.
%
% See wfn.m  --  Draws graph in Abramowitz & Stegun,
% Handbook of Mathematical Functions, p. 298

if nargin == 1, N=64; end                       % Default value for N
M=2*N; M2=2*M; k=[-M+1:1:M-1]';                 % M2=no. of sampling points
L=sqrt(N/sqrt(2));                              % Optimal choice of L
theta=k*pi/M; t=L*tan(theta/2);                 % Variables thetaand t
f=exp(-t.^2).*(L^2+t.^2); f=[0;f];              % function to be transformed
a=real(fft(fftshift(f)))/M2;                    % Coefficients of transform
a=flipud(a(2:N+1));                             % Reorder coefficients
nz=imag(z) <= 0;                                % Find im(z) <=0
z(nz)=conj(z(nz));                              % Use conj for above
Z=(L+i*z)./(L-i*z); p=polyval(a,Z);             % Polynomial evaluation
w=2*p./(L-i*z).^2+(1/sqrt(pi))./(L-i*z);        % Evaluate w(z)
w(nz)=2*exp(-(conj(z(nz)).^2)) - conj(w(nz));   % Handle im(z) <= 0
%if all(imag(z)==0), w=real(w); end             % Rtn real if real
```

Constants

```
function [w,cv,epso,u0,zo,k0,k1,kappap,lo]=cnstdg(f)
% This m-file contains the basic constants to be used by various
% m-files and functions
%
% f is input in GHz
% global EPSREL SIGMA
w=2*pi*f*1e9;
cv=2.99792458e8;
epso=(1/(4*pi))*1e7*(1/cv^2);
eps1=EPSREL;
u0=4*pi*1e-7;
zo=sqrt(u0/epso);
k0=w*sqrt(epso*u0);
epsr=(eps1-j*SIGMA./(w*epso));
k1=k0*sqrt(epsr);
kappap=-k0/sqrt(epsr+1);
lo=cv/(f*1e9);
```

Vertical Dipole

```
function [ez,er,hp]=dipg(f,d,rho,z)

%
% Electromagnetic fields from a vertical z-directed current element
% at a height, d, over a conducting dielectric plane (ground) calculated
% by the King/Sandler model. This formulation is that developed
% as equations 6, 7, and 8 of "The Electromagnetic Field of a Vertical Electric
% Dipole over the Earth or Sea", IEEE Trans. on Antennas and Propagation,
% March 1994, Vol 42 No. 3, page 383. It is the same as the King/Owens/Wu
% formulation. This formulation is that developed as equations 4.2.30-32 of
% "Lateral Electromagnetic Waves", Springer-Verlag, 1992, pp 293-297.
%
%    > f- frequency; rho- radial distance from the z-axis
%    < z- height of observer above ground plane (input as an array)
%    > ez,er,hp- field components at the observer, where the second letter
%    < designates the component -- z, r (rho), p (phi)
%
% The formulation is subject to |k1(ground)|>3|k2(air)|
%
[w,c,eps0,u0,zo,k2,k1,kappap,lo]=cnstdg(f);
%
```

```
% King, et. al assume an exp(-i*omega*time)dependency thus we convert k1
%
k1=conj(k1);
%N2=(k1/k2)^2;
k21=k2/k1;
%
% We assume a unit dipole
%
il=1;
r1=(rho^2+(z-d).^2).^.5;
r2=(rho^2+(z+d).^2).^.5;
sd=rho./r1;
sr=rho./r2;
cd=(z-d)./r1;
cr=(d+z)./r2;
p=(r2*k2^3/(2*k1^2)).*((k2*r2+k1*(z+d))./(k2*rho)).^2;
%
% The attenuation function less the exp(i*p) term - related to the
% error function is
%
Ferf=((1+i)/4)*werf(sqrt(i*p));
%
% Develop the terms for the field expressions
%
t1=w*u0*il/(2*pi*k2);
t11=-il/(2*pi);
t2=exp(i*k2*r1)/2;
t3=(i*k2./r1)-(1./r1.^2)-i./(k2*r1.^3);
t31=(i*k2./r1)-(1./r1.^2);
t4=(cd.^2).*((i*k2./r1)-(3./r1.^2)-(3*i)./(k2*r1.^3));
t41=((i*k2./r1)-(3./r1.^2)-(3*i)./(k2*r1.^3));
t5=exp(i*k2*r2)/2;
t6=(i*k2./r2)-(1./r2.^2)-i./(k2*r2.^3);
t61=(i*k2./r2)-(1./r2.^2);
t7=(cr.^2).*((i*k2./r2)-(3./r2.^2)-(3*i)./(k2*r2.^3));
t71=((i*k2./r2)-(3./r2.^2)-(3*i)./(k2*r2.^3));
t8=(2*t5*(k2^3)/k1).*((pi./(k2*r2)).^.5).*sr.*Ferf;
t81=((k2^3)/k1)*((pi./(k2*r2)).^.5).*Ferf;
t82=(2*t5.*(k2^3)/k1).*((pi./(k2*r2)).^.5).*Ferf;
%
% Calculate the fields
% ez=t1*(t2.*(t3-t4)+t5.*(t6-t7)-t8);
er=-t1*(t2.*sd.*cd.*t41+t5.*sr.*cr.*t71-k21*2*t5.*(sr.*t61-t81));
hp=t11*(t2.*sd.*t31+t5.*sr.*t61-t82);
```

Horizontal Dipole

```
function [ez,ep,er,hz,hp,hr]=dipgh(f,d,phi,rho,z)

%
%  Electromagnetic fields from a horizontally directed (perpendicular to z)
%  current element located in the phi=0 plane
%  at a height, d, over a conducting dielectric plane (ground) calculated
%  by the King/Owens/Wu formulation. This formulation is that developed
%  as equations 7.10.75, 7.10.80, 7.10.84, 7.10.92, 7.10.93 and 7.10.94 of
%  "Lateral Electromagnetic Waves", Springer-Verlag, 1992, pp 293-297.
%
%     > f- frequency(GHz); phi- angle about the z-axis,  rho- radial distance from
%     < the z-axis,  z- height of observer above ground plane (input as an array)
%     > ez,ep,er,hz,hp,hr- field components at the observer, where the second
%     < letter designates the component -- z, r (rho), p (phi)
%
%
%  The formulation is subject to |k1(ground)|>3|k2(air)|
%
[w,c,eps0,u0,zo,k2,k1,kappap,lo]=cnstdg(f);
%
%     King, et. al assume an exp(-i*omega*time)dependency thus we convert k1
%
k1=conj(k1);
%N2=(k1/k2)^2;
k21=k2/k1;
k2p=k2/rho;
%
% We assume a unit dipole
%
il=1;
cp=cos(phi);
sp=sin(phi);
r1=(rho^2+(z-d).^2).^.5;
r2=(rho^2+(z+d).^2).^.5;
sd=r1/rho;
sdo=1./sd;
sr=r2/rho;
sro=1./sr;
cd=(z-d)./r1;
cr=(d+z)./r2;
p=(r2*k2^3/(2*k1^2)).*((k2*r2+k1*(z+d))./(k2*rho)).^2;
```

```
%
% The attenuation function less the exp(i*p) term - related to the
% error function is
% Ferf=((1+i)/4)*werf(sqrt(i*p));
%
% Develop the terms for the field expressions
%
t1=w*u0*il*cp/(4*pi*k2);
t11=-w*u0*il*sp/(4*pi*k2);
t12=il*sp/(4*pi);
t13=il*cp/(4*pi);
t2=exp(i*k2*r1);
t32=(i*k2./r1)-(1./r1.^2)-i./(k2*r1.^3);
t3=(2./r1.^2)+2*i./(k2*r1.^3);
t31=(i*k2./r1)-(1./r1.^2);
t4=(cd.^2).*((i*k2./r1)-(3./r1.^2)-(3*i)./(k2*r1.^3));
t41=(cd).*((i*k2./r1)-(3./r1.^2)-(3*i)./(k2*r1.^3));
t5=exp(i*k2*r2);
t62=(i*k2./r2)-(1./r2.^2)-i./(k2*r2.^3);
t6=(2./r2.^2)+2*i./(k2*r2.^3);
t61=(i*k2./r2)-(1./r2.^2);
t7=(cr.^2).*((i*k2./r2)-(3./r2.^2)-(3*i)./(k2*r2.^3));
t71=(cr).*((i*k2./r2)-(3./r2.^2)-(3*i)./(k2*r2.^3));
t72=((1./r2.^2)+(3*i)./(k2*r2.^3)-3./((k2^2)*r2.^4));
t73=(cr.^2).*((i*k2./r2)-(6./r2.^2)-(15*i)./(k2*r2.^3));
t8=((k2^3)/k1)*((pi./(k2*r2)).^.5).*sr.*Ferf;
t81=((k2^3)/k1)*((pi./(k2*r2)).^.5).*Ferf;
t82=(2*t5*(k2^3)/k1).*((pi./(k2*r2)).^.5).*Ferf;
t83=((pi./(k2*r2)).^.5).*Ferf;
%
% Calculate the fields
%
ez=t1*(-t2.*sdo.*t41+t5.*sro.*t71-2*k21*t5.*(sro.*t61-t81));
er=t1*(t2.*(t3+t4)-t5.*(t6+t7-2*k21*t61+2*(k21^2)*(t62-t8)));
ep=t11*(t2.*t32-t5.*t62-t5.*(-2*k21*cr.*t61+2*(k21^2)*(t6+t7)...
   +2*i*k21^3*k2p*(sr.^2).*t83));
hr=t12*(t2.*cd.*t31-t5.*cr.*t61+2*k21*t5.*(t6+i*k21*k2p*(sr.^2).*t83+t7));
hp=t13*(t2.*cd.*t31-t5.*cr.*t61+2*k21*t5.*(t62-k21*(k2^2)*(sr).*t83));
hz=t12*(t2.*sdo.*t31-t5.*sro.*t61+2*sro.*t5.*(k21*t71(k21^2)*(t72+t73)));
```

Plot m-File for Fields

```
%
%  This m-file plots the fields over a conductive flat earth produced by an ideal
%  dipole placed a distance d above the earth. It compares the results from
%  a vertical and horizontal dipole.
%
%
%    Establish the problem conditions
%
%
%  EPSREL- Relative dielectric constant; SIGMA- Earth conductivity (S/m)
%
EPSREL=80;SIGMA=4;
global EPSREL SIGMA
%EPSREL=12;SIGMA=.4;
%EPSREL=8;SIGMA=.04;
%EPSREL=80;SIGMA=.004;
%EPSREL=2;SIGMA=.000;
%
%  Location of dipole (m)
%
d=2;
%
%  Location of observer, rho (m); phi (radians); z (m) ---> an array
%
rho=1000;
phi=pi/2;
z=.1*[1:1:30];
%
%  f- frequency in GHz
%
f=1.3;
%
%        Field normalization factor - one Watt radiated
%
[w,c,eps0,u0,zo,k2,k1,kappap,lo]=cnstdg(f);
Fn=sqrt(12*pi/((k2^2)*zo));
%
%       Horizontal dipole fields
%
[ez,ep,er,hz,hp,hr]=dipgh(f,d,phi,rho,z);
plot(Fn*abs(ep),z,'-b')
hold
```

```
%
%       Vertical dipole fields
%
[ezv,erv,hpv]=dipg(f,d,rho,z);
plot(Fn*abs(ezv),z,'-.r')
ts=Fn*abs(erv(1));
title('Vertical and Horizontal Ideal Dipole fields over Ground')
text(ts,z(19),['SIGMA = ',num2str(SIGMA),' S/m     EPSREL=
',num2str(EPSREL)])
text(ts,z(18),['Dipole height = ',num2str(d),' meters;   Frequency =
',num2str(f),' GHz'])
text(ts,z(17),['Range = ',num2str(rho),' meters'])
ylabel('Observer height - meters')
xlabel('Normalized field magnitude - V/m')
legend('Horizontal E-field, horizontal dipole','z-directed E-field,
vertical dipole')
hold
```

Fresnel Reflection Coefficients and Plots

```
function [rcomv,rcomh]=Fresnel1(f,psi)

%
% This routine calculates the Fresnel reflection coefficients for
% vertical and horizontal incident fields
%
% after Collin, "Antenna and Radiowave Propagation", page 345
%
% f-frequency in GHz;  psi- array of incident angles
%
% Code returns the arrays rcomv and rcomh, the vertical and horizontal
% complex reflection coefficients, respectively.
%
global EPSREL SIGMA
w=2*pi*f*1e9;
cv=2.99792458e8;
epso=(1/(4*pi))*1e7*(1/cv^2);
epsr=(EPSREL-j*SIGMA./(w*epso));
rcomv=(epsr*sin(psi)-sqrt(epsr-cos(psi).^2))./(epsr*sin(psi)+sqrt(epsr-cos(psi).^2));
rcomh=(sin(psi)-sqrt(epsr-cos(psi).^2))./(sin(psi)+sqrt(epsr-cos(psi).^2));

++++++++++++++++++++++++++++++++++++++++++++++++++++++++++++++++++++++++++++++++++++++++++++++++++++++++

%
```

```
% This m-file plots the reflection coefficient for vertical and horizontal
% fields over a homogeneous ground plane
%
%
% EPSREL- Relative dielectric constant; SIGMA- Earth conductivity (S/m)
%
EPSREL=80;SIGMA=4;
f=1.3;
global EPSREL SIGMA
psi=[pi/1000:pi/1000:pi/2];
[rcomv,rcomh]=Fresnel1(f,psi);
EPSREL=12;SIGMA=.4;
[rcomv1,rcomh1]=Fresnel1(f,psi);
EPSREL=8;SIGMA=.04;
[rcomv2,rcomh2]=Fresnel1(f,psi);
EPSREL=80;SIGMA=.004;
[rcomv3,rcomh3]=Fresnel1(f,psi);
EPSREL=2;SIGMA=.000;
[rcomv4,rcomh4]=Fresnel1(f,psi);

subplot(2,2,1),plot((180/pi)*psi,abs(rcomv),'k')
hold
axis([0,90,0,1])
xlabel('Incidence angle (degrees)')
ylabel('Reflection Coefficient')
%text(5,.8,['SIGMA = ',num2str(SIGMA),' S/m     EPSREL= ',num2str(EPSREL)])
subplot(2,2,1),plot((180/pi)*psi,abs(rcomv1),'r')
subplot(2,2,1),plot((180/pi)*psi,abs(rcomv2),'b')
subplot(2,2,1),plot((180/pi)*psi,abs(rcomv3),'g')
subplot(2,2,1),plot((180/pi)*psi,abs(rcomv4),'c')
hold

subplot(2,2,2),plot((180/pi)*psi,(180/pi)*angle(rcomv),'k')
hold
axis([0,90,-190,5])
xlabel('Incidence angle (degrees)')
ylabel('Phase')
subplot(2,2,2),plot((180/pi)*psi,(180/pi)*angle(rcomv1),'r')
subplot(2,2,2),plot((180/pi)*psi,(180/pi)*angle(rcomv2),'b')
subplot(2,2,2),plot((180/pi)*psi,(180/pi)*angle(rcomv3),'g')
subplot(2,2,2),plot((180/pi)*psi,-(180/pi)*angle(rcomv4),'c')
hold

subplot(2,2,3),plot((180/pi)*psi,abs(rcomh),'k')
```

```
hold
axis([0,90,.5,1])
xlabel('Incidence angle (degrees)')
ylabel('Reflection Coefficient')
subplot(2,2,3),plot((180/pi)*psi,abs(rcomh1),'r')
subplot(2,2,3),plot((180/pi)*psi,abs(rcomh2),'b')
subplot(2,2,3),plot((180/pi)*psi,abs(rcomh3),'g')
subplot(2,2,3),plot((180/pi)*psi,abs(rcomh4),'c')
hold

subplot(2,2,4),plot((180/pi)*psi,(180/pi)*angle(rcomh),'k')
hold
axis([0,90,170,200])
xlabel('Incidence angle (degrees)')
ylabel('Phase')
subplot(2,2,4),plot((180/pi)*psi,(180/pi)*angle(rcomh1),'r')
subplot(2,2,4),plot((180/pi)*psi,(180/pi)*angle(rcomh2),'b')
subplot(2,2,4),plot((180/pi)*psi,(180/pi)*angle(rcomh3),'g')
subplot(2,2,4),plot((180/pi)*psi,(180/pi)*angle(rcomh4),'c')
hold
```

Distribution

Admnstr
Defns Techl Info Ctr
ATTN DTIC-OCP
8725 John J Kingman Rd Ste 0944
FT Belvoir VA 22060-6218

DARPA
ATTN S Welby
3701 N Fairfax Dr
Arlington VA 22203-1714

Ofc of the Secy of Defns
ATTN ODDRE (R&AT)
The Pentagon
Washington DC 20301-3080

Ofc of the Secy of Defns
ATTN OUSD(A&T)/ODDR&E(R) R J Trew
3080 Defense Pentagon
Washington DC 20301-7100

AMCOM MRDEC
ATTN AMSMI-RD W C McCorkle
Redstone Arsenal AL 35898-5240

US Army TRADOC
Battle Lab Integration & Techl Dirctrt
ATTN ATCD-B
ATTN ATCD-B J A Klevecz
FT Monroe VA 23651-5850

US Military Acdmy
Mathematical Sci Ctr of Excellence
ATTN MADN-MATH MAJ M Huber
Thayer Hall
West Point NY 10996-1786

Dir for MANPRINT
Ofc of the Deputy Chief of Staff for Prsnnl
ATTN J Hiller
The Pentagon Rm 2C733
Washington DC 20301-0300

SMC/CZA
2435 Vela Way Ste 1613
El Segundo CA 90245-5500

TECOM
ATTN AMSTE-CL
Aberdeen Proving Ground MD 21005-5057

US Army ARDEC
ATTN AMSTA-AR-TD
Bldg 1
Picatinny Arsenal NJ 07806-5000

US Army Info Sys Engrg Cmnd
ATTN AMSEL-IE-TD F Jenia
FT Huachuca AZ 85613-5300

US Army Natick RDEC Acting Techl Dir
ATTN SBCN-T P Brandler
Natick MA 01760-5002

US Army Natl Ground Intllgnc Ctr
ATTN IAFSTC-RMA T Caldwell
220 Seventh St NE
Charlottesville VA 22901-5396

US Army Nuc & Chem Agcy
ATTN MONA-NU R Pfeffer
7150 Heller Loop Rd Ste 101
Springfield VA 22150

US Army Simulation Train & Instrmntn Cmnd
ATTN AMSTI-CG M Macedonia
ATTN J Stahl
12350 Research Parkway
Orlando FL 32826-3726

US Army TACOM
ATTN ATSTA-OE E Di Vito
Warren MI 48397-5000

US Army Tank-Automtv Cmnd RDEC
ATTN AMSTA-TR J Chapin
Warren MI 48397-5000

Nav Air Warfare Ctr Aircraft Div
ATTN E3 Div S Frazier Code 5.1.7
Unit 4 Bldg 966
Patuxent River MD 20670-1701

Distribution (cont'd)

Nav Rsrch Lab
ATTN Code 6650 T Wieting
4555 Overlook Ave SW
Washington DC 20375-5000

Nav Surfc Warfare Ctr
ATTN Code B07 J Pennella
17320 Dahlgren Rd Bldg 1470 Rm 1101
Dahlgren VA 22448-5100

Nav Surfc Warfare Ctr
ATTN Code F-45 D Stoudt
ATTN Code F-45 S Moran
ATTN Code J-52 W Lucado
Dahlgren VA 22448-5100

Air Force Rsrch Lab (Phillips Ctr)
ATTN AFRL/WST W Walton
ATTN AFRL W L Baker Bldg 413
ATTN WSM P Vail
3550 Aberdeen Ave SE
Kirtland NM 87112-5776

CIA
ATTN OSWR J F Pina
Washington DC 20505

Federal Communications Commission
Office of Eng and Technl
ATTN Rm 7-A340 R Chase
445 12th Stret SW
Washington DC 20554

Hicks & Assoc Inc
ATTN G Singley III
1710 Goodrich Dr Ste 1300
McLean VA 22102

Pacific Northwest Natl Lab
ATTN K8-41 R Shippell
PO Box 999
Richland WA 99352

Palisades Inst for Rsrch Svc Inc
ATTN E Carr
1745 Jefferson Davis Hwy Ste 500
Arlington VA 22202-3402

Sparta
ATTN R O'Connor
4901 Corporate Dr Ste 102
Huntsville AL 35805-6257

Director
US Army Rsrch Lab
ATTN AMSRL-RO-D JCI Chang
ATTN AMSRL-RO-EN W D Bach
PO Box 12211
Research Triangle Park NC 27709

US Army Rsrch Lab
ATTN AMSRL-DD J M Miller
ATTN AMSRL-D D R Smith
ATTN AMSRL-CI-AI-R Mail & Records Mgmt
ATTN AMSRL-CI-AP Techl Pub (2 copies)
ATTN AMSRL-CI-LL Techl Lib (2 copies)
ATTN AMSRL-SE-DP M Litz
ATTN AMSRL-SE-DP R A Kehs (3 copies)
ATTN AMSRL-SE-DS J Miletta (10 copies)
ATTN AMSRL-SE-DS J Tatum (5 copies)
ATTN AMSRL-SE-DS M Berry
ATTN AMSRL-SE-DS W O Coburn
Adelphi MD 20783-1197

REPORT DOCUMENTATION PAGE

Form Approved
OMB No. 0704-0188

1. AGENCY USE ONLY *(Leave blank)*

2. REPORT DATE
February 2001

3. REPORT TYPE AND DATES COVERED
Summary, Oct 99 to Sept 00

4. TITLE AND SUBTITLE Propagation of Electromagnetic Fields Over Flat Earth

5. FUNDING NUMBERS
DA PR: AH94
PE: 62705A

6. AUTHOR(S) Joseph R. Miletta

7. PERFORMING ORGANIZATION NAME(S) AND ADDRESS(ES)
U.S. Army Research Laboratory
Attn: AMSRL-SE-DS email: jmiletta@arl.army.mil
2800 Powder Mill Road
Adelphi, MD 20783-1197

8. PERFORMING ORGANIZATION REPORT NUMBER
ARL-TR-2352

9. SPONSORING/MONITORING AGENCY NAME(S) AND ADDRESS(ES)
U.S. Army Research Laboratory
2800 Powder Mill Road
Adelphi, MD 20783-1197

10. SPONSORING/MONITORING AGENCY REPORT NUMBER

11. SUPPLEMENTARY NOTES
ARL PR: 0NE6YY
AMS code: 622705.H94

12a. DISTRIBUTION/AVAILABILITY STATEMENT Approved for public release; distribution unlimited.

12b. DISTRIBUTION CODE

13. ABSTRACT *(Maximum 200 words)*

This report looks at the interaction of radiated electromagnetic fields with earth ground in military or law-enforcement applications of high-power microwave (HPM) systems. For such systems to be effective, the microwave power density on target must be maximized. The destructive and constructive scattering of the fields as they propagate to the target will determine the power density at the target for a given source. The question of field polarization arises in designing an antenna for an HPM system. Should the transmitting antenna produce vertically, horizontally, or circularly polarized fields? Which polarization maximizes the power density on target? This report provides a partial answer to these questions. The problems of calculating the reflection of uniform plane wave fields from a homogeneous boundary and calculating the fields from a finite source local to a perfectly conducting boundary are relatively straightforward. However, when the source is local to a general homogeneous plane boundary, the solution cannot be expressed in closed form. An approximation usually of the form of an asymptotic expansion results. Calculations of the fields are provided for various source and target locations for the frequencies of interest. The conclusion is drawn that the resultant vertical field from an appropriately oriented source antenna located near and above the ground can be significantly larger than a horizontally polarized field radiated from the same location at a 1.3 GHz frequency at observer locations near and above the ground.

14. SUBJECT TERMS Antenna, ground interaction

15. NUMBER OF PAGES
33

16. PRICE CODE

17. SECURITY CLASSIFICATION OF REPORT	18. SECURITY CLASSIFICATION OF THIS PAGE	19. SECURITY CLASSIFICATION OF ABSTRACT	20. LIMITATION OF ABSTRACT
Unclassified	Unclassified	Unclassified	UL

NSN 7540-01-280-5500

Standard Form 298 (Rev. 2-89)
Prescribed by ANSI Std. Z39-18
298-102